Sampling Theorem for Surface Profiling by White-Light Interferometry

OGAWA HIDEMITSU
Department of Computer Science, Tokyo Institute of Technology
HIRABAYASHI AKIRA
Department of Computer Science and Systems Engineering, Yamaguchi University
KITAGAWA KATSUICHI
Electronics Division, Toray Engineering Co.,Ltd.

Abstract

White-light interferometry is a technique to measure surface topology of objects such as semiconductors, liquid crystal displays (LCDs), plastic films, and precision machinery parts. We devise a generalized sampling theorem for white-light interferometry. It reconstructs a square envelope function of an interference fringe directly from sampled values of the interference fringe, not from those of the square envelope function itself. The reconstruction formula requires only arithmetical calculations, no transcendental calculations except for only one cosine function. It has been installed in a commercial system that achieved the world's fastest vertical scanning speed, $42\mu\mathrm{m}/s$, 6-14 times faster than conventional methods.

1 Introduction

We propose a generalized sampling theorem for surface profiling by white-light interferometry. It is a technique to measure surface topology of objects such as semiconductors, liquid crystal displays (LCDs), plastic films, and precision machinery parts [1–7,12–14]. The proposed sampling theorem has the following interesting feature. It reconstructs a square envelope function, $r(z)$, of an interference fringe, $f(z)$, from sampled values of $f(z)$, not $r(z)$.

There exists a similar problem, where a function should be reconstructed from sampled values of its filtered function [8, 9]. However, our problem is its reverse. It is a problem of reconstructing a nonlinearly filtered function $r(z)$ from sampled values of the original function $f(z)$.

The proposed sampling theorem is very simple. It requires only arithmetical calculations, no transcendental calculations except for only one cosine function.

It has been installed in a commercial system [13] which achieved the world's fastest vertical scanning speed, 6-14 times faster than those of the conventional systems [12, 14].

2 Surface Profiling by White-Light Interferometry

In this section, surface profiling by white-light interferometry is outlined. Figure 1 shows a basic set up of a white-light interferometer used for surface profiling. An incoherent white-light source illuminates a beam-splitter through a narrowband optical filter, whose center wavelength and bandwidth are λ_c and $2\lambda_b$, respectively. For example, for a typical filter $\lambda_c = 600nm$ and $\lambda_b = 30nm$. The beam-splitter transmits one portion of the beam, indicated by the dashed line, to a surface of an object being observed and the other portion, indicated by the dotted line, to a reference mirror. These two beams are recombined and interfere. The resultant beam intensity is observed by a charge-coupled device (CCD) video camera which has, for example, 512×480 detectors. Each of them corresponds to a point on the object surface.

As the interferometer is scanned along the vertical axis, z-axis, the intensity observed by one of the detectors is varied. The intensity along the z-axis is shown in Figure 2 by a dotted line. The graph is called the white-light interference fringe or simply the interfer-

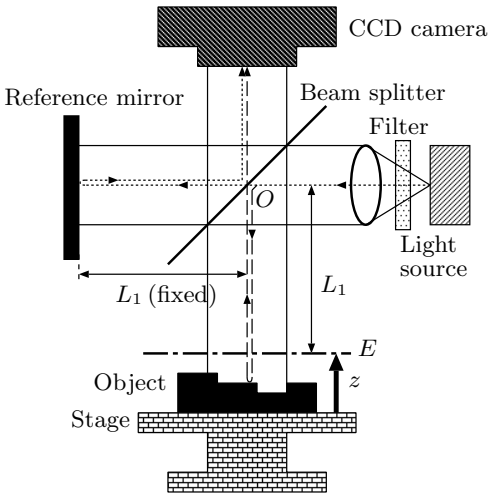

Figure 1: Basic setup of a white-light interferometer.

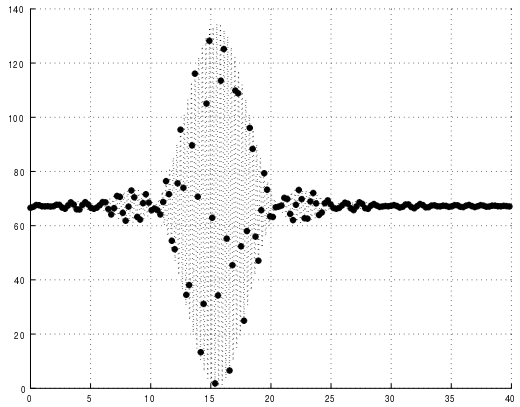

Figure 2: The white-light interference fringe $g(z)$ and its sampled values shown by '•'.

ence fringe. It shifts to the right in Figure 2 if the height of the object surface at a point is high, while it shifts to the left if the height is low. Hence, the maximum position of the fringe provides the height of the point on the surface.

A CCD camera outputs the intensity of the interference fringe, for example, every 1/30 second. Hence, we can utilize only discrete sampled values of the interference fringe as shown by '•' in Figure 2. From these sampled values, we have to estimate the maximum position of the interference fringe. Therefore, sampling theory naturally plays an important role.

3 Mathematical Model of the Interference Fringe

We shall describe a mathematical model of the interference fringe following [5, 6]. In Figure 1, L_1 is a distance of the reference mirror from the point O where the beam from the light source passes through the beam splitter. E is a virtual plane whose distance from the point O is L_1. z is the distance of the plane E from the stage. It is referred to as the height of the interferometer.

As mentioned before, each CCD detector corresponds to a point (x, y) on the object surface, where x and y are the transverse coordinates on the stage of the interferometer. The height of the surface of the object at the point (x, y) is denoted by z_p.

A model of the interference fringe is given as

$$g(z) = f(z) + C, \tag{1}$$

where C is a constant and $f(z)$ is a function defined by

$$f(z) = \int_{k_l}^{k_u} \psi(k) \cos 2k(z - z_p)\, dk. \tag{2}$$

In Eq.(2), k is the angular wavenumber defined by

$$k = \frac{2\pi}{\lambda}, \tag{3}$$

where λ is the wavelength. In the interval of integration, k_l and k_u are

$$k_l = \frac{2\pi}{\lambda_c + \lambda_b}, \quad k_u = \frac{2\pi}{\lambda_c - \lambda_b}. \tag{4}$$

$\psi(k)$ is an energy distribution of the incident beam to the CCD detector with respect to k. It is restricted to the interval $[k_l, k_u]$ by the optical filter:

$$\psi(k) = 0 \quad (k < k_l\,,\, k > k_u). \tag{5}$$

Since $f(z)$ is band-limited as shown later in Eq.(16), $f(z)$ and $g(z)$ are continuous. Hence, we can discuss sampled values of $g(z)$ and we have

Lemma 1 ([5]) *The interference fringe $g(z)$ has the maximum only at $z = z_p$, i.e., it holds that for $z \neq z_p$*

$$g(z) < g(z_p). \tag{6}$$

Lemma 1 guarantees that the maximum position of the interference fringe $g(z)$ agrees with the height z_p of the point on the object surface. In practice, however, it is hard to obtain the maximum position z_p from $g(z)$, because $g(z)$ has high-frequency components. In order to cope with this problem, we use the square envelope function of the interference fringe. The details will be discussed in the following sections.

4 Square Envelope Function

In order to overcome the problem mentioned at the end of the previous section, we shall introduce a function, $r(z)$, which has the following three properties:

(i) $r(z)$ has the maximum only at $z = z_p$, i.e., it holds that $r(z) < r(z_p)$ for $z \neq z_p$.

(ii) $r(z)$ is smoother than the interference fringe.

(iii) $r(z)$ can be reconstructed from sampled values of the interference fringe.

Let k_c be any fixed positive real number. Let us define

$$m_c(z) = \int_{k_l}^{k_u} \psi(k) \cos 2\{k(z - z_p) - k_c z\} dk, \tag{7}$$

$$m_s(z) = -\int_{k_l}^{k_u} \psi(k) \sin 2\{k(z - z_p) - k_c z\} dk. \tag{8}$$

Then, the interference fringe $f(z)$ is expressed by

$$f(z) = m_c(z) \cos 2k_c z + m_s(z) \sin 2k_c z. \tag{9}$$

Eq.(9) yields

$$f(z) = m(z) \cos\{2k_c z - \alpha(z)\}, \tag{10}$$

where

$$m(z) = \sqrt{\{m_c(z)\}^2 + \{m_s(z)\}^2}, \tag{11}$$

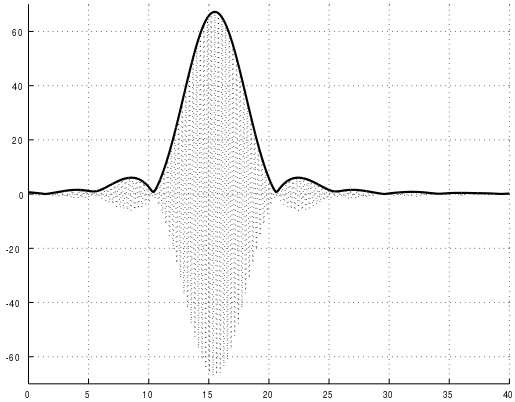

Figure 3: An example of the interference fringe $f(z)$ and its envelope $m(z)$.

$$\alpha(z) = \begin{cases} \tan^{-1}\dfrac{m_s(z)}{m_c(z)} & (m_c(z) \neq 0), \\ \pi/2 & (m_c(z) = 0,\ m_s(z) > 0), \\ -\pi/2 & (m_c(z) = 0,\ m_s(z) < 0). \end{cases}$$

The value of $\tan^{-1}(x)$ is restricted to the interval $(-\pi/2, \pi/2)$.

The function $f(z)$ and $m(z)$ are shown in Figure 3 by dotted and solid lines, respectively. We can see that the function $m(z)$ is the envelope of the interference fringe $f(z)$.

Now, we shall introduce the square envelope functions of $f(z)$.

Definition 1 *The function $r(z)$ defined by*

$$r(z) = \{m_c(z)\}^2 + \{m_s(z)\}^2 \tag{12}$$

is called the square envelope function of the interference fringe $f(z)$.

The following two lemmas guarantee that the square envelope function $r(z)$ has the properties (i) and (ii) mentioned at the beginning of this section. In the next section, it will be shown that the square envelope function has the property (iii), too.

Lemma 2 *The square envelope function $r(z)$ is independent of k_c. It has the maximum at only $z = z_p$, i.e., it holds that for any $z \neq z_p$*

$$r(z) < r(z_p). \tag{13}$$

Lemma 2 implies that the square envelope function has the property (i).

We shall show that $r(z)$ has the property (ii). Let $\hat{f}(\omega)$ be the Fourier transform of $f(z)$:

$$\hat{f}(\omega) = \int_{-\infty}^{\infty} f(z) e^{-i\omega z} dz. \tag{14}$$

From Eq.(2), we have

$$\hat{f}(\omega) = \frac{\pi}{2} e^{-i\omega z_p} \psi\left(\frac{|\omega|}{2}\right). \tag{15}$$

Eq.(15) means that $f(z)$ is a bandpass signal such that

$$\hat{f}(\omega) = 0 \quad (|\omega| < \omega_l\ ,\ |\omega| > \omega_u), \tag{16}$$

where

$$\omega_l = 2k_l, \quad \omega_u = 2k_u. \tag{17}$$

Lemma 3 *The square envelope function $r(z)$ is a lowpass signal such that*

$$\hat{r}(\omega) = 0 \quad (|\omega| > \omega_u - \omega_l), \tag{18}$$

where $\hat{r}(\omega)$ is the Fourier transform of $r(z)$.

Eqs.(17) and (4) imply that $\omega_u - \omega_l < \omega_l$ if and only if $\lambda_c > 3\lambda_b$. In this case, $r(z)$ is smoother than $f(z)$ because of Eqs.(16) and (18). For example, if $\lambda_c = 600nm$ and $\lambda_b = 30nm$, then $\omega_l = 19.95[1/\mu\text{m}]$, $\omega_u - \omega_l = 2.10[1/\mu\text{m}]$. Hence, $r(z)$ is much smoother than $f(z)$, and the square envelope function has the property (ii).

5 Sampling Theorem for Square Envelope Functions

In this section, we shall show that the square envelope function $r(z)$ has the property (iii) mentioned in the last section. That is, we shall provide a formula of reconstructing $r(z)$ from sampled values of the interference fringe $f(z)$. Since $r(z)$ is defined by functions $m_c(z)$ and $m_s(z)$ in Eq.(12), we shall start with sampling theorems for these functions.

5.1 Sampling Theorems for $m_c(z)$ and $m_s(z)$

We first show that $m_c(z)$ and $m_s(z)$ are band-limited signals of the lowpass type. Let $\hat{m}_c(\omega)$ and $\hat{m}_s(\omega)$ be the Fourier transforms of $m_c(z)$ and $m_s(z)$, respectively. Let

$$\omega_c = 2k_c. \tag{19}$$

Lemma 4 *$m_c(z)$ and $m_s(z)$ are lowpass signals such that*

$$\hat{m}_c(\omega) = \hat{m}_s(\omega) = 0 \quad (|\omega| > \omega_b), \tag{20}$$

where ω_b is

$$\omega_b = \max\{|\omega_c - \omega_l|, |\omega_c - \omega_u|\} \tag{21}$$

$$= \begin{cases} \omega_u - \omega_c & (\omega_c \leq \frac{\omega_u + \omega_l}{2}), \\ \omega_c - \omega_l & (\omega_c > \frac{\omega_u + \omega_l}{2}). \end{cases} \tag{22}$$

Lemma 4 implies that $m_c(z)$ and $m_s(z)$ are completely reconstructed from their sampled values if the sampling interval is less than or equal to the Nyquist interval Δ_b defined by

$$\Delta_b = \frac{\pi}{\omega_b}. \tag{23}$$

These sampled values are, however, not available directly.

Then, we shall discuss the problem of obtaining sampled values of $m_c(z)$ and $m_s(z)$ from sampled values of $f(z)$. It can be divided into the following two subproblems:

(i) Can we obtain sampled values of $m_c(z)$ and $m_s(z)$ from sampled values of $f(z)$?

(ii) If (i) is possible, is the sampling interval used in (i) consistent with Δ_b in Eq.(23)?

We first discuss the problem (i). The basic idea is that, if $\sin 2k_c z$ or $\cos 2k_c z$ in Eq.(9) vanishes at $z = z_0$, we can obtain $m_c(z_0)$ or $m_s(z_0)$ from $f(z_0)$, respectively. Let Δ_c be a sampling interval such that

$$\Delta_c = \frac{\pi}{\omega_c}. \tag{24}$$

It follows from Eqs.(24) and (19) that $\sin 2k_c z_0 = 0$ if and only if $z_0 = n\Delta_c$ for any fixed integer n. In this case, $\cos\{2k_c(n\Delta_c)\} = (-1)^n$, and Eq.(9) yields

$$m_c(n\Delta_c) = (-1)^n f(n\Delta_c). \tag{25}$$

Similarly, $\cos 2k_c z_0 = 0$ if and only if $z_0 = (n + \frac{1}{2})\Delta_c$, and we have

$$m_s((n + \tfrac{1}{2})\Delta_c) = (-1)^n f((n + \tfrac{1}{2})\Delta_c). \tag{26}$$

Owing to Eqs.(25) and (26), the problem (i) has been settled in a very simple way.

Now, the problem (ii) reduces to the problem of obtaining a condition for $\Delta_c \le \Delta_b$. Note that both Δ_b and Δ_c are functions of ω_c because of Eqs.(22), (23), and (24). The following Lemma 5 provides a necessary and sufficient condition for $\Delta_c \le \Delta_b$.

Lemma 5 *It holds that*

$$\Delta_c \le \Delta_b \tag{27}$$

if and only if ω_c given by Eq.(19) satisfies

$$\omega_c \ge \tfrac{1}{2}\,\omega_u. \tag{28}$$

If we let $\omega_c = (\omega_u + \omega_l)/2$, then Eq.(28) holds. In this case, if $\lambda_c = 600nm$ and $\lambda_b = 30nm$, we have $\Delta_c = 0.299nm$ and $\Delta_b = 2.99nm$. Δ_b is 10 times as large as Δ_c. This example means that we can reduce sample points $\{n\Delta_c\}_{n=-\infty}^{\infty}$ and $\{(n + \frac{1}{2})\Delta_c\}_{n=-\infty}^{\infty}$ in Eqs.(25) and (26) when we apply the Someya-Shannon sampling theorem [10, 11] to $m_c(z)$ and $m_s(z)$.

Consider the case that for a positive integer M, every M sample points among $\{n\Delta_c\}_{n=-\infty}^{\infty}$ and $\{(n + \frac{1}{2})\Delta_c\}_{n=-\infty}^{\infty}$ are used. In this case, the problem (ii) reduces to the problem of obtaining a condition for $M\Delta_c \le \Delta_b$. The following Lemma 6 provides a necessary and sufficient condition for this relation.

Lemma 6 *For any fixed $\omega_c \ge \frac{1}{2}\,\omega_u$, it holds that*

$$M\Delta_c \le \Delta_b \tag{29}$$

if and only if M satisfies

$$\begin{cases} 1 \le M \le \dfrac{\omega_c}{\omega_u - \omega_c} & (\omega_c \le \dfrac{\omega_u + \omega_l}{2}), \\ 1 \le M \le \dfrac{\omega_c}{\omega_c - \omega_l} & (\omega_c > \dfrac{\omega_u + \omega_l}{2}). \end{cases} \tag{30}$$

By using the integer M in Lemma 6, we can reduce sample points $\{n\Delta_c\}_{n=-\infty}^{\infty}$ and $\{(n+\frac{1}{2})\Delta_c\}_{n=-\infty}^{\infty}$. Let I_c and I_s be any fixed nonnegative integers less than M. Let

$$z_n^{(c)} = (nM + I_c)\Delta_c, \tag{31}$$

$$z_n^{(s)} = \{(nM + I_s) + \tfrac{1}{2}\}\Delta_c. \tag{32}$$

I_c and I_s control initial points of $z_n^{(c)}$ and $z_n^{(s)}$, i.e., $z_0^{(c)} = I_c\Delta_c$ and $z_0^{(s)} = (I_s + \frac{1}{2})\Delta_c$. We can impose the restrictions $0 \le I_c, I_s \le M - 1$ without loss of generality.

For these sample points, Eqs.(25) and (26) yield

$$m_c(z_n^{(c)}) = (-1)^{nM+I_c} f(z_n^{(c)}), \tag{33}$$

$$m_s(z_n^{(s)}) = (-1)^{nM+I_s} f(z_n^{(s)}). \tag{34}$$

Then, we have

Theorem 1 (*Sampling Theorems for $m_c(z)$ and $m_s(z)$*) *For any fixed $\omega_c \ge \frac{1}{2}\,\omega_u$, let Δ_c be a sampling interval defined by Eq.(24), and M be a positive integer such that Eq.(30) holds. Let I_c and I_s be nonnegative integers less than M. Let $\{z_n^{(c)}\}_{n=-\infty}^{\infty}$ and $\{z_n^{(s)}\}_{n=-\infty}^{\infty}$ be sample points defined by Eqs.(31) and (32). Then, it holds that*

$$m_c(z) = (-1)^{I_c} \sum_{n=-\infty}^{\infty} (-1)^{nM} f(z_n^{(c)}) \mathrm{sinc} \frac{z - z_n^{(c)}}{M\Delta_c}, \tag{35}$$

$$m_s(z) = (-1)^{I_s} \sum_{n=-\infty}^{\infty} (-1)^{nM} f(z_n^{(s)}) \mathrm{sinc} \frac{z - z_n^{(s)}}{M\Delta_c}, \tag{36}$$

where $\mathrm{sinc}(z)$ *is a function defined by*

$$\mathrm{sinc}(z) = \begin{cases} \dfrac{\sin \pi z}{\pi z} & (z \ne 0), \\ 1 & (z = 0). \end{cases} \tag{37}$$

5.2 Sampling Theorem for $r(z)$

Based on Theorem 1, we shall derive a sampling theorem for the square envelope function $r(z)$. Remember that the optical filter in the interferometer is characterized by the center wavelength λ_c and the bandwidth $2\lambda_b$ as mentioned in Section 2. Since λ_c and λ_b are more familiar than ω_l and ω_u for practical engineers, we shall use λ_c and λ_b from now on. These parameters are mutually related by

$$\omega_l = \frac{4\pi}{\lambda_c + \lambda_b}, \quad \omega_u = \frac{4\pi}{\lambda_c - \lambda_b} \tag{38}$$

because of Eqs.(4) and (17).

In order to reconstruct the square envelope function $r(z)$ by using Eqs.(35) and (36), we need both $\{z_n^{(c)}\}_{n=-\infty}^{\infty}$ and $\{z_n^{(s)}\}_{n=-\infty}^{\infty}$. The total sample points $\{z_n^{(c)}, z_n^{(s)}\}_{n=-\infty}^{\infty}$ are not equally spaced in general. However, uniform sampling is more useful in practical applications. We shall derive such a sampling theorem for square envelope functions. We discuss the case where $I_c = 0$ in this paper. It can be easily extended to the general I_c. Since $I_c = 0$, between two consecutive sample points $z_n^{(c)}$ and $z_{n+1}^{(c)}$ there is exactly one sample point $z_n^{(s)}$. Hence, uniform sampling can be achieved when

$$z_{n+1}^{(c)} - z_n^{(s)} = z_n^{(s)} - z_n^{(c)}. \tag{39}$$

Eq.(39) holds if and only if

$$I_s = \tfrac{1}{2}(M-1). \tag{40}$$

Eqs.(32) and (40) yield

$$z_n^{(s)} = \tfrac{1}{2}(2n+1)M\Delta_c. \tag{41}$$

Hence, if we let

$$\Delta = \tfrac{1}{2}M\Delta_c, \tag{42}$$

$$z_n = n\Delta, \tag{43}$$

then

$$z_n^{(c)} = z_{2n}, \quad z_n^{(s)} = z_{2n+1}, \tag{44}$$

and we have

Theorem 2 (*Sampling Theorem for Square Envelope Functions*) *Let I be a nonnegative integer such that*

$$0 \le I \le \frac{\lambda_c - \lambda_b}{2\lambda_b}, \tag{45}$$

and Δ be a real number which satisfies

$$\frac{I}{4}(\lambda_c + \lambda_b) \le \Delta \le \frac{I+1}{4}(\lambda_c - \lambda_b). \tag{46}$$

Let $\{z_n\}_{n=-\infty}^{\infty}$ be sample points defined by Eq.(43). Then, it holds that

1. *When z is a sample point z_j,*

$$r(z_j) = \{f(z_j)\}^2 + \frac{4}{\pi^2}\left\{\sum_{n=-\infty}^{\infty}\frac{f(z_{j+2n+1})}{2n+1}\right\}^2. \tag{47}$$

2. *When z is not any sample point,*

$$r(z) = \frac{2\Delta^2}{\pi^2}\left[(1-\cos\frac{\pi z}{\Delta})\left\{\sum_{n=-\infty}^{\infty}\frac{f(z_{2n})}{z-z_{2n}}\right\}^2 + (1+\cos\frac{\pi z}{\Delta})\left\{\sum_{n=-\infty}^{\infty}\frac{f(z_{2n+1})}{z-z_{2n+1}}\right\}^2\right]. \tag{48}$$

Note that Eq.(47) needs only arithmetical calculations. Eq.(48) needs arithmetical calculations except for only one cosine function calculation. It does not need no other transcendental calculations.

λ_c and λ_b are the characteristics of the optical filter used in an interferometer. Eqs.(45) and (46) mean that the characteristics of the optical filter determine the sampling interval Δ completely.

The following is a direct consequence of Theorem 2.

Corollary 1 *The maximum, Δ_{max}, of the sampling interval Δ is given by*

$$\Delta_{max} = \frac{\lambda_c - \lambda_b}{4}\left(\left\lfloor\frac{\lambda_c - \lambda_b}{2\lambda_b}\right\rfloor + 1\right), \tag{49}$$

where $\lfloor x \rfloor$ is the maximum integer which does not exceed a real number x.

If an optical filter of $\lambda_c = 600nm$ and $\lambda_b = 30nm$ is used, Δ_{max} is 1.425μm. It is much wider than sampling intervals used in conventional systems. For example, in the systems produced by Veeco Instruments Inc. and Zygo Corporation, sampling intervals are 0.24μm and 0.10μm, respectively [12, 14]. Δ_{max} is about 6 and 14 times wider than intervals of these systems.

Eq.(46) means that an infinite number of sampling intervals Δ are available. Each of them can be used for complete reconstruction of $r(z)$. There is no diference among them. In practical applications, however, only finite number of sample points are available, and Eqs.(47) and (48) are truncated. In such a situation, each sampling interval causes different effects. A wider sampling interval allows us faster scan of the interferometer in Figure 1, while it causes larger truncation error. Hence, for choosing the sampling interval Δ, we have to take scanning speed and the truncation error into account at the same time.

6 New Surface Profiling Algorithm and Surface Profiler

By using Theorem 2, we propose a new surface profiling algorithm. Theorem 2 assumes that (a) an infinite number of sampled values can be used, and (b) sampled values $f(z_n)$ of the interference fringe $f(z)$ are available. In practical applications, however, (a) only a finite number of sampled values can be used, and (b) only sampled values $g(z_n)$ of the interference fringe $g(z)$ in Eq.(1) are available.

For the problem (a), we truncate the infinite series in Eqs.(47) and (48) from $n = 0$ to $N-1$. For the problem (b), the sampled values $f(z_n)$ is approximated by

$$f_n = g(z_n) - \hat{C}, \tag{50}$$

where $\hat{C}$ is an estimate of C in Eq.(1). For example, the average of $\{g(z_n)\}_{n=0}^{N-1}$ can be used as $\hat{C}$:

$$\hat{C} = \frac{1}{N}\sum_{n=0}^{N-1} g(z_n). \tag{51}$$

The surface profiling algorithm based on these process is named the EES algorithm after *Estimation of the square Envelope function by Sampling theorem*. This algorithm has been installed in a commercial system [13], which is shown in Figure 4. Figure 5 shows a three-dimensional image of IC bumps obtained by the surface profiler.

If an optical filter of $\lambda_c = 600nm$ and $\lambda_b = 30nm$ is used, the maximum scanning speed of the system is $42.75\mu\mathrm{m}/s$. It is the world's fastest scan speed. We can make the scan speed faster by changing the optical filter,

In order to evaluate the accuracy of the profiler, we measured the surface profile of a step height standard of 9.947μm. Its three-dimensional image is shown in Figure 6. The difference between the averages of estimated values of z_p for the lower part and the higher part is 9.933μm. The relative error is 0.13%, which shows the good performance of the surface profiler.

Figure 4: Photograph of a surface profiler in which the EES algorithm has been installed.

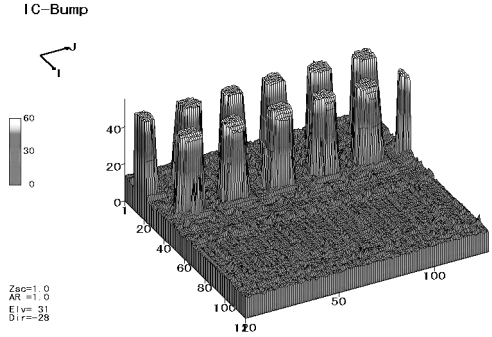

Figure 5: Three-dimensional image of IC bumps obtained by the surface profiler shown in Figure 4.

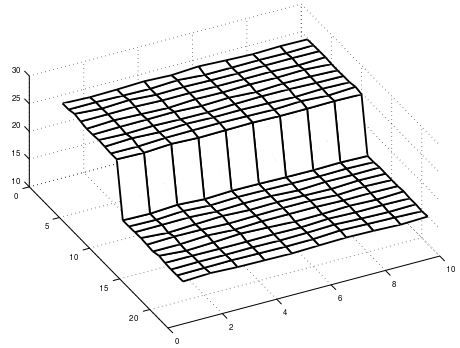

Figure 6: Three-dimensional image of a step height standard of 9.947μm obtained by the surface profiler.

References

[1] P.J. Caber, Interferometric profiler for rough surfaces, *Applied Optics*, **32**(19), 3438–3441, 1993.

[2] S.S.C. Chim and G.S. Kino, Correlation microscope, *Optics letters*, **15**(10), 579–581, 1990.

[3] S.S.C. Chim and G.S. Kino, Three-dimensional image realization in interference microscopy, *Applied Optics*, **31**(14), 2550–2553, 1992.

[4] P. de Groot and L. Deck, Surface profiling by analysis of white-light interferograms in the spatial frequency domain, *Journal of Modern Optics*, **42**(2), 389–401, 1995.

[5] A. Hirabayashi, H. Ogawa, T. Mizutani, K. Nagai, and K. Kitagawa, Fast surface profiling by white-light interferometry using a sampling theorem for band-pass signals, *Trans. Society of Instrument and Control Engineers*, **36**(1), 16–25, 2000, (in Japanese).

[6] G.S. Kino and S.S.C. Chim, Mirau correlation microscope, *Applied Optics*, **29**(26), 3775–3783, 1990.

[7] K.G. Larkin, Efficient nonlinear algorithm for envelope detection in white light interferometry, *Journal of Optical Society of America*, **13**(4), 832–843, 1996.

[8] H. Ogawa, A generalized sampling theorem, *Electronics and Communications in Japan, Part.3*, **72**(3), 97–105, 1989, It is translated from IEICE Trans. on Information and Systems, **J71-A**(2), 163-170, 1988.

[9] A. Papoulis, *Signal Analysis*, McGraw-Hill, New York, 1977.

[10] C.E. Shannon, Communications in the presence of noise, *Proc. IRE*, **37**, 10–21, 1949.

[11] I. Someya, *Waveform Transmission*, Shukyosha, Tokyo, 1949.

[12] Veeco Instruments Inc. Catalog, No. NTS-1-0500, *Wyko NT Series Ultrafast Optical Profilers*, 2000.

[13] http://www.cable-net.ne.jp/corp/torayins/index-eng.html.

[14] http://www.zygo.com/.